

Measurement of Raman gain for various crystals by a cavity method

© Ya.A. Kochukov^{1,3}, P.D. Kharitonova¹, D.N. Seleznev¹, K.A. Gubina^{1,3}, D.P. Tereshchenko¹, N.A. Khokhlov², E.S. Barkanova², A.G. Papashvili¹, V.E. Shukshin¹, I.S. Voronina¹, S.N. Smetanin^{1,3}

¹ Prokhorov Institute of General Physics, Russian Academy of Sciences, Moscow, Russia

² Mendelev University of Chemical Technology, Moscow, Russia

³ National University of Science and Technology „MISIS“, Moscow, Russia

e-mail: ko4ukovura@yandex.ru

Received September 12, 2024

Revised January 15, 2025

Accepted January 16, 2025

A cavity method has been developed to provide a simple measurement of the Raman gain for various crystals. Formulas for processing experimental results are theoretically justified taking into account the pump pulse duration and the Gaussian beam profile. Under the action of a nanosecond laser with a wavelength of 1064 nm, the Raman gain was measured for a number of crystals: SrMoO₄, Sr(MoO₄)_{0.8}(WO₄)_{0.2}, Sr_{0.86}Ba_{0.14}MoO₄, Sr_{0.9}Ba_{0.1}MoO₄ and LiNa₅Mo₉O₃₀. For the well-known SrMoO₄ Raman crystal, the result obtained is consistent with the literature data (5.6 cm/GW). For SrMoO₄-based solid solutions, a decrease in the Raman gain compared to that for SrMoO₄ correlates with an increase in the width of the vibrational mode line. For the first time, stimulated Raman scattering was obtained in Sr_{0.86}Ba_{0.14}MoO₄, Sr_{0.9}Ba_{0.1}MoO₄ and LiNa₅Mo₉O₃₀ crystals with the comparable Raman gain of 2.4–2.5 cm/GW under pumping with a wavelength of 1064 nm.

Keywords: Stimulated Raman scattering, Raman gain, optical cavity, generation threshold.

DOI: 10.61011/EOS.2025.01.60566.7060-24

1. Introduction

The stimulated Raman scattering (SRS) in crystals is a simple and easy way of laser radiation frequency transformation that doesn't need any sustaining of phase synchronism [1]. By selecting the SRS-crystals of various combination frequencies allows finding the appropriate shift of the laser radiation frequency for a specific purpose, e.g., for the fluorescent microscopy of live tissues [2]. Another important characteristic that determines the successful use of a SRS-crystal is the Raman gain, but any available measurement data for various crystals obtained by different methods are limited or have a high error. For example, the direct measurement method — the single-pass amplifier method [3,4] — is technically the most complex, requiring consideration of spatial, temporal and spectral overlap of pump radiation and Stokes SRS-radiation, so it is rarely used in practice. In most cases the measurements are made by a technically more simple method — method of a generator [5–10]. Here, in order to obtain SRS-generation in one pass of a SRS-crystal, the pumping intensity has to be greatly increased, and in order to prevent radiation breakdown of the SRS-crystal, it is necessary to shorten the pulses of exciting laser radiation using picosecond pumping lasers. However, in this case, the SRS regime in crystals with picosecond phase relaxation times becomes transient, which leads to the need to use complex indirect estimates, leading to a high error in measuring the steady-state Raman

gain [9,10]. In [11], an original express-method was used to measure the Raman gain of CaCO₃ crystal — a cavity method. The cavity method consists in placing the SRS crystal in the cavity, which lowered the threshold of SRS generation compared to the SRS-crystal threshold radiation breakdown under the action of nanosecond pumping pulses.

The present work is devoted to the development of the cavity method to provide a more accurate measurement of Raman gain of various crystals. The formulae for processing experimental results take into account the duration of the pump pulse and the Gaussian beam profile. The Raman gain was measured for both, the known SRS-crystal of SrMoO₄, and for the new SRS-crystals of Sr(MoO₄)_{0.8}(WO₄)_{0.2}, Sr_{0.86}Ba_{0.14}MoO₄, Sr_{0.9}Ba_{0.1}MoO₄ and LiNa₅Mo₉O₃₀.

2. Theoretical underpinning of the cavity method

As it was noted in the review by N. Blombergen [12], the gain of SRS-laser, like any other laser, at the generation threshold should be equal to the cavity losses, which underlies the cavity method for measuring the Raman gain. However, in this way, only relative values of Raman gain were previously obtained as a function of the pump wavelength for a diamond crystal [13]. Absolute measurements require taking into account the duration of the pumping pulse, since in SRS-lasers, unlike lasers with population inversion, the amplification stops at the end of

the pumping pulse. At the same time, it is advisable to use the easy-to-implement pump radiation nanosecond pulses which ensure a steady-state of SRS regime in crystals and are longer than the SRS laser cavity round trip time with a cavity length below 10 cm.

The cavity method for measuring the Raman gain, which takes into account the duration of the pumping pulse, proposed in [11], is based on the plane-wave model of SRS in the cavity described in [14]. There is also a more accurate model using the focused Gaussian beam approximation [15], which justifies the determination of the effective pumping intensity.

To theoretically underpin this cavity method, we present here the formula derived for determining the Raman gain in the approximation of a collimated Gaussian beam sufficient to describe the SRS in a cavity. Here we are based on a well-known model of steady-state SRS amplification [16]:

$$\begin{aligned} \frac{dI_S(z, r)}{dz} &= g_R I_p(z, r) I_S(z, r) - k_S I_S(z, r), \\ \frac{dI_p(z, r)}{dz} &= -g_R \frac{\lambda_p}{\lambda_S} I_p(z, r) I_S(z, r) - k_p I_p(z, r), \end{aligned} \quad (1)$$

where g_R — the determined Raman gain of the SRS-laser active medium; $I_p(z, r)$ and $I_S(z, r)$ — intensities of the pumping radiation and Stokes SRS-radiation depending on the longitudinal (z) and transverse (r) coordinates; k_p and k_S — pumping radiation and SRS-radiation loss coefficients, λ_p and λ_S — wavelengths of pumping radiation and SRS-radiation.

In the approximation of a collimated Gaussian beam, the pump radiation and SRS-radiation beams have a Gaussian profile with a constant beam radius, and the dependence of the pumping radiation intensity on the longitudinal coordinate at SRS-threshold can be neglected:

$$\begin{aligned} I_S(z, r) &= P_S(z) \frac{2}{\pi \cdot r_S^2} \exp\left(-2\frac{r^2}{r_S^2}\right), \\ I_p(z, r) &\approx P_p \frac{2}{\pi \cdot r_p^2} \exp\left(-2\frac{r^2}{r_p^2}\right), \end{aligned} \quad (2)$$

where $P_{p,S} = \int_0^\infty I_{p,S} 2\pi r dr$ — power of pumping radiation and SRS-radiation; $r_{p,S}$ — radius of the pumping radiation and SRS-radiation beams $1/e^2$.

By integrating the first equation of the system of equations (1) along the transverse coordinate $\left(\int_0^\infty 2\pi r dr\right)$, taking into account the expressions (2) we obtain the SRS-radiation power equation:

$$\frac{dP_S(z)}{dz} = g_R P_p P_S(z) \frac{2}{\pi r_p^2 + \pi r_S^2} - k_S P_S(z). \quad (3)$$

To describe a multi-pass SRS in an external (relative to the pumping laser) double-mirror cavity, we proceed to a

kinetic analysis that can be used when the pumping pulse time is many times longer than the cavity round trip time:

$$\frac{n_R}{\mu c} \frac{dP_S(t)}{dt} = g_R P_p P_S(t) \frac{2}{\pi r_p^2 + \pi r_S^2} - k_S P_S(t), \quad (4)$$

where $\mu = n_R L_R / L_c$ — coefficient of laser filling with an active medium (ratio of optical length of active medium to the optical length of cavity) [17], n_R — refractive index of SRS-laser active medium, L_R — length of SRS-laser active medium, $L_c = L_g - L_R + L_R n_R$ — optical length of SRS-laser cavity, L_g — geometrical length of SRS-laser cavity, c — light velocity in vacuum,

$$k_S = \frac{1}{L_R} \ln \frac{1}{\sqrt{T_R^2 R_S^{in} R_S^{out}}} \quad (5)$$

— SRS-laser cavity loss coefficient, T_R — SRS-laser transmission coefficient per one pass at SRS-radiation wavelength, $R_S^{in, out}$ — reflectance of input (in) and output (out) mirror of SRS-laser cavity at SRS-radiation wavelength. The radiation power of pumping inside the active medium of a SRS-laser with an external double-mirror cavity can be defined as

$$P_p = \frac{E_p}{\tau_p} (1 - R_p^{in}) \sum_{i=1}^N \left[(R_p^{in} R_p^{out})^{i-1} + (R_p^{in})^{i-1} (R_p^{out})^i \right], \quad (6)$$

where E_p — pumping radiation pulse energy at SRS-laser input, τ_p — duration of the pumping radiation pulse, $R_p^{in, out}$ — reflectance of the input (in) and output (out) mirrors of the cavity of SRS-laser at the pump wavelength, $N \approx \tau_p / \tau_c$ — number of cavity round trips during pumping, $\tau_c = 2L_c / c$ — cavity round trip time. Under $R_p^{in} \approx 0$ formula (6) is simplified to $P_p \approx (1 + R_p^{out}) E_p / \tau_p$, as in paper [15].

Solution of equation (4) at the end of pumping pulse duration can be written as

$$P_S(\tau_p) = P_S(0) e^G, \quad (7)$$

where increment of exponential Raman gain is defined as

$$G = \left(g_R I_p L_R - \ln \frac{1}{\sqrt{T_R^2 R_S^{in} R_S^{out}}} \right) \frac{c \tau_p}{L_c}. \quad (8)$$

Here $I_p = P_p / S$ — effective pumping intensity, $S = (\pi r_p^2 + \pi r_S^2) / 2$ — effective beam section. We obtain the expression for the effective pumping intensity $I_p = 2P_p / (\pi r_p^2 + \pi r_S^2)$.

The SRS threshold condition can be defined as [18] $G = 25$, then, equating the expression (8) by this value, we obtain the desired formula for the Raman gain

$$g_R = \frac{1}{L_p^{th} L_R} \left(\frac{25 L_c}{\tau_p c} + \ln \frac{1}{\sqrt{T_R^2 R_S^{in} R_S^{out}}} \right), \quad (9)$$

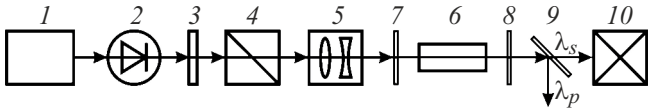


Figure 1. Experimental optical setup: 1 — pumping laser; 2 — Faraday isolator; 3 — half-wave plate; 4 — polarizer; 5 — focusing system; 6 — SRS-crystal; 7 — cavity input mirror; 8 — cavity output mirror; 9 — mirror filter; 10 — recorder.

Which coincides with that obtained in the plane-wave approximation [11]. Here, the threshold value of the effective pumping intensity inside the SRS medium is determined by the formula

$$I_p^{th} = \frac{E_p^{th}}{\tau_p S} (1 - R_p^{in}) \sum_{i=1}^N \left[(R_p^{in} P_p^{out})^{i-1} + (R_p^{in})^{i-1} (R_p^{out})^i \right], \quad (10)$$

where E_p^{th} — measured threshold of pumping radiation pulse energy at SRS-laser input. In the case of a very long pumping pulse, the first term in parentheses of (9) can be ignored, then we come to the original formula from the review of N.Blombergen [12], valid in case of continuous pumping [15].

3. Taking measurements

Experimental optical setup is shown in Fig. 1. Radiation of the pumping laser 1 passed through Faraday insulator 2 for isolation between the pumping laser and SRS-laser. Next, a half-wave plate 3 and a polarizer 4 were installed to smoothly regulate the energy of the pumping radiation pulse E_p at the input of SRS laser when the half-wave plate 3 is rotated. Further, the focusing system 5 is installed based on a pair of lenses, in the focus of which the SRS crystal 6 under study is placed. The SRS-laser consisted of SRS-crystal 6 placed in the optical cavity based on plane mirrors 7 and 8, with the distance between them of $L_g = 9.5$ cm. The input mirror 7 had reflectance $R_{1064} = 3.5\%$, $R_{1175} = 99.8\%$ and $R_{1183} = 99.9\%$ at the wavelengths of 1064, 1175 and 1183 nm respectively, and the output mirror 8 — $R_{1064} = 83.7\%$, $R_{1175} = 80.2\%$ and $R_{1183} = 79.6\%$. At the output of SRS-laser a mirror filter 9 is installed, reflecting the pumping radiation of (1064 nm) and passing the SRS-radiation of (1175–1183 nm). The SRS radiation passed through the filter 9 was sent to the recorder 10, which was used as a visible-range spectrometer with a frequency doubler, or as a radiation energy meter.

Measurements were performed for the SRS-crystals SrMoO_4 ($L_R = 5.7$ cm, $n_R = 1.9$), $\text{Sr}(\text{MoO}_4)_{0.8}(\text{WO}_4)_{0.2}$ ($L_R = 7.0$ cm, $n_R = 1.9$), $\text{Sr}_{0.86}\text{Ba}_{0.14}\text{MoO}_4$ ($L_R = 4.4$ cm, $n_R = 1.9$), $\text{Sr}_{0.9}\text{Ba}_{0.1}\text{MoO}_4$ ($L_R = 6.5$ cm, $n_R = 1.9$) and $\text{LiNa}_5\text{Mo}_9\text{O}_{30}$ ($L_R = 5.7$ cm, $n_R = 1.8$). The crystal SrMoO_4 is a well-known and efficient SRS-medium [19–22], crystal $\text{Sr}(\text{MoO}_4)_{0.8}(\text{WO}_4)_{0.2}$ was used only once for SRS earlier [23], and the remaining three crystals —

$\text{Sr}_{0.86}\text{Ba}_{0.14}\text{MoO}_4$, $\text{Sr}_{0.9}\text{Ba}_{0.1}\text{MoO}_4$ and $\text{LiNa}_5\text{Mo}_9\text{O}_{30}$ — are the new SRS-media where SRS in this study was obtained for the first time. The first three crystals had anti-reflective coatings on the plane-parallel ends, the last two — had no such coatings. All crystals were cut along the crystallooptic axis Y .

According to the polarized Raman spectroscopy performed, the solid solutions $\text{Sr}(\text{MoO}_4)_{0.8}(\text{WO}_4)_{0.2}$, $\text{Sr}_{0.86}\text{Ba}_{0.14}\text{MoO}_4$ and $\text{Sr}_{0.9}\text{Ba}_{0.1}\text{MoO}_4$, as well as the original crystal SrMoO_4 [21], should have been pumped in $Y(\text{ZZ})Y$ configuration which is distinguished by a higher intensity of the symmetrical stretch vibrations mode of the anion group compared to $Y(\text{XX})Y$. It should be noted that in the anion solid solution $\text{Sr}(\text{MoO}_4)_{0.8}(\text{WO}_4)_{0.2}$ this mode ($\nu_R = 887 \text{ cm}^{-1}$) have a spectral width of $\Delta\nu_R = 4.3 \text{ cm}^{-1}$, which is 1.7 times higher than in SrMoO_4 . In the cation solid solutions $\text{Sr}_{0.86}\text{Ba}_{0.14}\text{MoO}_4$ and $\text{Sr}_{0.9}\text{Ba}_{0.1}\text{MoO}_4$ the broadening of this mode ($\nu_R = 888 \text{ cm}^{-1}$) is even higher — up to $\Delta\nu_R = 6.5 \text{ cm}^{-1}$ (in 2.6 times) which is explained by a combination of stretch vibrations with the closely spaced frequencies in SrMoO_4 ($\nu_R = 887 \text{ cm}^{-1}$) and BaMoO_4 ($\nu_R = 892 \text{ cm}^{-1}$) [24]. The last crystal — $\text{LiNa}_5\text{Mo}_9\text{O}_{30}$ — in contrast, should be pumped in $Y(\text{XX})Y$ configuration, for which the intensity of the symmetrical stretch vibrations mode of the anion group $\nu_R = 947 \text{ cm}^{-1}$ is higher than for $Y(\text{ZZ})Y$.

A single-mode YAG:Nd^{3+} laser was used as a pumping laser with electro-optical Q-switching generating radiation pulses with a duration of 15 ns with a pulse energy of 130 mJ at a wavelength of 1064 nm. With the help of a focusing system, the radius of the pump radiation beam in the SRS-crystal was set as large as possible, equal to $r_p = 1.9$ mm at the level of $1/e^2$, limited by the aperture of SRS-crystal, so that it could be considered unchanged over the entire length of the SRS-crystal and to minimize diffraction losses on the flat mirrors of the SRS-laser cavity (the Rayleigh length of the pumping beam in air $z_R \approx 1$ m was by an order of magnitude longer than the length of SRS-laser cavity). In this paper, we implemented an express method in which we used flat cavity mirrors so that the radius of the SRS-beam was the largest and closest to the radius of the pumping beam ($r_p \approx r_s$), then, we may assume $S \approx \pi r_p^2$, as in the plane-wave approximation [11]. In fact, the measured value r_s was only 9% less than r_p (within the measurement error).

First, using the pumping laser for each of the SRS-crystals their transmission value T_R was measured after removal of mirrors 7 and 8 from the setup in Fig. 1. It was $T_R = 93, 92, 95, 77$ and 79% for the crystals SrMoO_4 , $\text{Sr}(\text{MoO}_4)_{0.8}(\text{WO}_4)_{0.2}$, $\text{Sr}_{0.86}\text{Ba}_{0.14}\text{MoO}_4$, $\text{Sr}_{0.9}\text{Ba}_{0.1}\text{MoO}_4$ and $\text{LiNa}_5\text{Mo}_9\text{O}_{30}$ respectively. The low transmission of the last two crystals is due to the absence of anti-reflective coatings on them. Further, the mirrors 7 and 8 were installed and aligned. Upon receiving the SRS-generation, the ends of each SRS crystal were slightly misaligned so that they did not contribute to the generation.

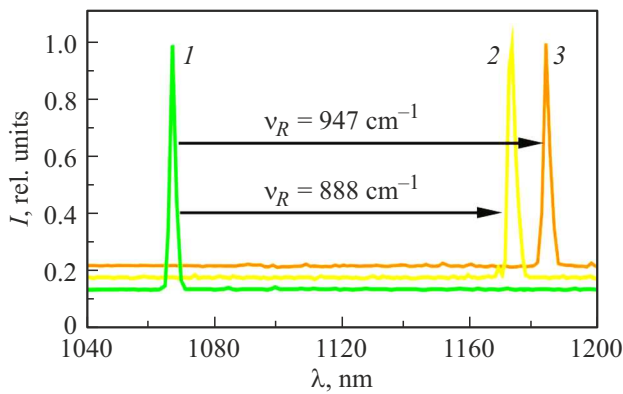


Figure 2. Spectra of pumping radiation (curve 1) and SRS-radiation for the new SRS-crystals $\text{Sr}_{0.86}\text{Ba}_{0.14}\text{MoO}_4$ (curve 2) and $\text{LiNa}_5\text{Mo}_9\text{O}_{30}$ (curve 3).

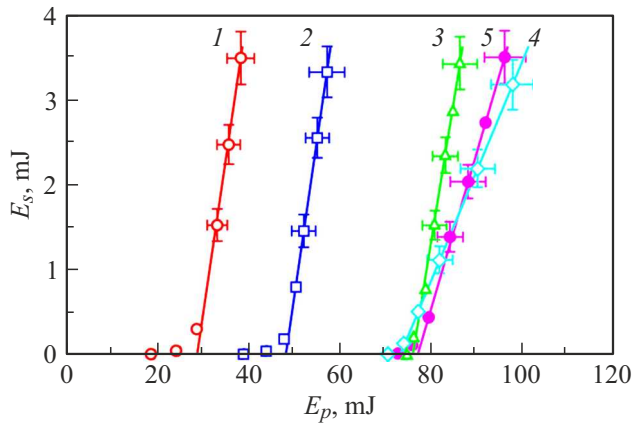


Figure 3. SRS-radiation pulse energy versus pumping pulse energy for crystals SrMoO_4 (curve 1), $\text{Sr}(\text{MoO}_4)_{0.8}(\text{WO}_4)_{0.2}$ (curve 2), $\text{Sr}_{0.86}\text{Ba}_{0.14}\text{MoO}_4$ (curve 3), $\text{Sr}_{0.9}\text{Ba}_{0.1}\text{MoO}_4$ (curve 4) and $\text{LiNa}_5\text{Mo}_9\text{O}_{30}$ (curve 5).

Results of measuring the characteristics of SRS-crystals: ν_R — frequency of the stretch vibrations mode for anion group, $\Delta\nu_R$ — its spectral width, g_R — Raman gain at $\lambda_p = 1064$ nm

SRS-crystal	ν_R, cm^{-1}	$\Delta\nu_R, \text{cm}^{-1}$	$g_R, \text{cm/GW}$
SrMoO_4	887	2.5	5.6 ± 0.2
$\text{Sr}(\text{MoO}_4)_{0.8}(\text{WO}_4)_{0.2}$	887	4.3	2.9 ± 0.1
$\text{Sr}_{0.86}\text{Ba}_{0.14}\text{MoO}_4$	888	6.5	2.5 ± 0.1
$\text{Sr}_{0.9}\text{Ba}_{0.1}\text{MoO}_4$	888	6.5	2.4 ± 0.1
$\text{LiNa}_5\text{Mo}_9\text{O}_{30}$	947	4.0	2.4 ± 0.1

Fig. 2 illustrates the measured spectra of pumping radiation (curve 1) and SRS-radiation for new SRS-crystals $\text{Sr}_{0.86}\text{Ba}_{0.14}\text{MoO}_4$ (curve 2) and $\text{LiNa}_5\text{Mo}_9\text{O}_{30}$ (curve 3). The SRS-radiation wavelengths were $\lambda_s = 1175$ and 1183 nm for crystals $\text{Sr}_{0.86}\text{Ba}_{0.14}\text{MoO}_4$ and $\text{LiNa}_5\text{Mo}_9\text{O}_{30}$, respectively. For the remaining crystals (SrMoO_4 ,

$\text{Sr}(\text{MoO}_4)_{0.8}(\text{WO}_4)_{0.2}$ and $\text{Sr}_{0.9}\text{Ba}_{0.1}\text{MoO}_4$) the spectra and wavelengths of SRS-radiation were equivalent to those presented for $\text{Sr}_{0.86}\text{Ba}_{0.14}\text{MoO}_4$, i.e. they had approximately the same frequency shift $\nu_R = 887\text{--}888 \text{ cm}^{-1}$, characteristic for the symmetric stretching of tetrahedral anion complex MoO_4 of the original SrMoO_4 crystal [9]. Crystal $\text{LiNa}_5\text{Mo}_9\text{O}_{30}$ provided a high frequency shift $\nu_R = 947 \text{ cm}^{-1}$, corresponding to the symmetric stretching of octahedral anion complex MoO_6 of this crystal [25].

Figure 3 shows the experimental dependences of SRS-radiation pulse energy on the pumping pulse energy for all studied crystals. Linear approximation of the measurement results at the intersection with X-axis gave the desired pumping energy thresholds E_p^{th} : 29 ± 1 mJ for SrMoO_4 , 49 ± 2 mJ for $\text{Sr}(\text{MoO}_4)_{0.8}(\text{WO}_4)_{0.2}$, 76 ± 3 mJ for $\text{Sr}_{0.86}\text{Ba}_{0.14}\text{MoO}_4$, 74 ± 3 mJ for $\text{Sr}_{0.9}\text{Ba}_{0.1}\text{MoO}_4$, 77 ± 3 mJ for $\text{LiNa}_5\text{Mo}_9\text{O}_{30}$. When substituting these values into formulae (9) and (10) the values of Raman gain are obtained for all studied crystals, which are listed in the table.

From the table we may see that the obtained value ($g_R = 5.6 \pm 0.2 \text{ cm/GW}$) for the known crystal SrMoO_4 is consistent with the previous measurement made by generator method ($g_R = 5.6 \text{ cm/GW}$) [9]. In the anion solid solution of $\text{Sr}(\text{MoO}_4)_{0.8}(\text{WO}_4)_{0.2}$ the Raman gain ($g_R = 2.9 \pm 0.1 \text{ cm/GW}$) turned out to be 1.9 times lower, while in the cation solid solutions of $\text{Sr}_{0.86}\text{Ba}_{0.14}\text{MoO}_4$ ($g_R = 2.5 \pm 0.1 \text{ cm/GW}$) and $\text{Sr}_{0.9}\text{Ba}_{0.1}\text{MoO}_4$ ($g_R = 2.4 \pm 0.1 \text{ cm/GW}$) — about 2.3 times less than for SrMoO_4 . This correlates with an increase in the spectral width of the vibrational mode ($\Delta\nu_R$) in solid solutions compared to SrMoO_4 , which is described above (see also the table). Due to a relatively narrow line of the vibrational mode ($\Delta\nu_R = 4 \text{ cm}^{-1}$) the Raman gain in the new SRS-crystal $\text{LiNa}_5\text{Mo}_9\text{O}_{30}$ turned out to be quite high ($g_R = 2.4 \pm 0.1 \text{ cm/GW}$) and comparable with that for the represented solid solutions based on SrMoO_4 . It should be stressed that the obtained values g_R relate to the pumping wavelength of 1064 nm. As the pumping wavelength increases the Raman gain goes down [3,4,13].

4. Conclusion

Thus, a cavity method was developed to provide a universal measurement of Raman gain for various crystals. The formulae for processing experimental findings allowed for the pumping pulse duration and the Gaussian beam profile. The Raman gain was measured for a number of SRS-crystals when pumped with a nanosecond laser with a wavelength of 1064 nm. For the known crystal SrMoO_4 the obtained data are in good agreement with literature data (5.6 cm/GW). For solid solutions based on SrMoO_4 , a decrease in Raman gain compared with that for SrMoO_4 correlates with an increase in the spectral width of the vibrational mode. For the first time, the SRS was obtained in crystals $\text{Sr}_{0.86}\text{Ba}_{0.14}\text{MoO}_4$, $\text{Sr}_{0.9}\text{Ba}_{0.1}\text{MoO}_4$

and $\text{LiNa}_5\text{Mo}_9\text{O}_{30}$ with comparable coefficient for their Raman gain 2.4–2.5 cm/GW when pumped with a 1064 nm wavelength pulse.

Funding

This study was supported financially by grant No. 24-12-00448 from the Russian Science Foundation.

Conflict of interest

The authors declare that they have no conflict of interest.

References

- [1] T.T. Basiev, V.V. Osiko. *Rus. Chem. Rev.*, **75** (10), 847 (2006). DOI: 10.1070/RC2006v075n10ABEH003626.
- [2] E.P. Perillo, J.W. Jarrett, Y.-L. Liu, A. Hassan, D.C. Fernee, J.R. Goldak, A. Bonteanu, D.J. Spence, H.-C. Yeh, A.K. Dunn. *Light: Science & Appl.*, **6**, e17095 (2017). DOI: 10.1038/lsa.2017.95
- [3] V.A. Lisinetskii, S.V. Rozhok, D.N. Bus'ko, R.V. Chulkov, A.S. Grabtchikov, V.A. Orlovich, T.T. Basiev, P.G. Zverev. *Laser Phys. Lett.*, **2** (8), 396 (2005). DOI: 10.1002/lapl.200510007
- [4] A. Sabella, D.J. Spence, R.P. Mildren. *IEEE J. Quantum Electron.*, **51** (12), 1000108 (2015). DOI: 10.1109/JQE.2015.2503404
- [5] A.Z. Grasyuk, S.V. Kurbasov, L.L. Losev, A.P. Lutsenko, A.A. Kaminskii, V.B. Semenov. *Quantum Electron.*, **28** (2), 162 (1998). DOI: 10.1070/QE1998v028n02ABEH001162.
- [6] A.A. Kaminskii, H.J. Eichler, K. Ueda, N.V. Klassen, B.S. Redkin, L.E. Li, J. Findeisen, D. Jaque, J. Garcia-Sole, J. Fernandez, R. Balda. *Appl. Opt.*, **38** (21), 4533 (1999). DOI: 10.1364/AO.38.004533
- [7] A.A. Kaminskii, K. Ueda, H.J. Eichler, Y. Kuwano, H. Kouta, S.N. Bagaev, Th.H. Chyba, J.C. Barnes, G.M.A. Gad, T. Murai, J. Lu. *Opt. Commun.*, **194**, 201 (2001). DOI: 10.1016/S0030-4018(01)01274-3
- [8] H.-L. Zhou, Q.-H. Zhang, B. Wang, X.-G. Xu, Zh.-P. Wang, X. Sun, F. Zhang, L.-S. Zhang, B.-A. Liu, X.-X. Chai. *Chin. Phys. B*, **24** (4), 044206 (2016). DOI: 10.1088/1674-1056/24/4/044206
- [9] T.T. Basiev, P.G. Zverev, A.Ya. Karasik, V.V. Osiko, A.A. Sobol', D.S. Chinaev. *J. Exp. Theor. Phys.*, **99**, 934 (2004). DOI: 10.1134/1.1842874.
- [10] S.N. Smetanin, *Opt. Spectrosc.*, **121** (3), 395 (2016). DOI: 10.1134/S0030400X1608021X.
- [11] S.N. Smetanin, M. Jelínek, D.P. Tereshchenko, V. Kubeček. *Optics Express*, **26** (18), 22637 (2018). DOI: 10.1364/OE.26.022637
- [12] N. Bloembergen. *Amer. J. Phys.*, **35** (11), 989 (1967). DOI: 10.1119/1.1973774
- [13] V.G. Savitski, S. Reilly, A.J. Kemp. *IEEE J. Quantum Electron.*, **49** (2), 218 (2013). DOI: 10.1109/JQE.2012.2237505
- [14] T.T. Basiev, M.N. Basieva, A.V. Gavrilov, M.N. Ershkov, L.I. Ivleva, V.V. Osiko, S.N. Smetanin, A.V. Fedin. *Quantum Electron.*, **40** (8), 710 (2010). DOI: 10.1070/QE2010v040n08ABEH014376.
- [15] V.A. Lisinetskii, A.S. Grabtchikov, P.A. Apanasevich, M. Schmitt, B. Kuschner, S. Schlücker, V.A. Orlovich. *J. Raman Spectrosc.*, **37** (1-3), 421 (2006). DOI: 10.1002/jrs.1447
- [16] O. Kitzler, A. McKay, D.J. Spence, R.P. Mildren. *Optics Express*, **23** (7), 8590 (2015). DOI: 10.1364/OE.23.008590
- [17] L.V. Tarasov. *Fizika protsessov v generatorakh kogerentnogo opticheskogo izlucheniya* (Radio i svyaz, M., 1981), p. 354 (in Russian).
- [18] A. Penzkofer, A. Laubereau, W. Kaiser. *Prog. Quantum Electron.*, **6** (2), 55 (1979). DOI: 10.1016/0079-6727(79)90011-9
- [19] A.A. Kaminskii, S.N. Bagaev, K. Ueda, K. Takaichi, H.J. Eichler. *Crystallography Reports*, **47** (4), 653 (2002). DOI: 10.1134/1.1496066.
- [20] H. Yu, Zh. Li, A.J. Lee, J. Li, H. Zhang, J. Wang, H.M. Pask, J.A. Piper, M. Jiang. *Opt. Lett.*, **36** (4), 579 (2011). DOI: 10.1364/OL.36.000579
- [21] M. Frank, S.N. Smetanin, M. Jelínek, D. Vyhliďal, A.A. Kopalkin, V.E. Shukshin, L.I. Ivleva, P.G. Zverev, V. Kubeček. *Opt. Laser Technol.*, **111**, 129 (2019). DOI: 10.1016/j.optlastec.2018.09.045
- [22] S.N. Smetanin, D. P. Tereshchenko, A.G. Papashvili, E.V. Shashkov, E.A. Peganov, K.A. Gubina, V.E. Shukshin, S.A. Solokhin, M.N. Ershkov, E.E. Dunaeva, I.S. Voronina, L.I. Ivleva. *Bull. Lebedev Physics Institute*, **50** (suppl. 9), S984 (2023). DOI: 10.3103/S1068335623210108.
- [23] D.P. Tereshchenko, S.N. Smetanin, A.G. Papashvili, K.A. Gubina, Yu.A. Kochukov, S.A. Solokhin, M.N. Ershkov, E.V. Shashkov, V.E. Shukshin, L.I. Ivleva, E.E. Dunaeva, I.S. Voronina. *Technical Physics*, **69** (5), 1427 (2024). DOI: 10.1134/S1063784224040431.
- [24] T.T. Basiev, A.A. Sobol, Yu.K. Voronko, P.G. Zverev. *Opt. Mater.*, **15**, 205 (2000). DOI: 10.1016/S0925-3467(00)00037-9
- [25] X. Du, Z. Gao, F. Liu, X. Guo, X. Wang, Y. Sun, X. Tao. *CrystEngComm*, **22**, 7716 (2020). DOI: 10.1039/D0CE01129K

Translated by T.Zorina